The control of combustion instability: A perspective

K. R. Sreenivasan[†] and S. Raghu*

Mason Laboratory, P.O. Box 208286, Yale University, New Haven, CT 06520, USA
*Present address: Bowles Fluidics, Columbia, MD 21045, USA

This article provides our perspective on the problem of active control of combustion instability. It makes no claim to complete or historically accurate survey, but attempts to put our past work in the context of existing literature. Starting with an equation for the energy of a general type of infinitesimal disturbance[1], we argue that the perturbation energy can be mitigated (or enhanced) by suitable addition of heat, mass, or body forces, along with species generation. We show that these principles work well in a number of simple experimental realizations, and highlight the application for a large combustion tunnel.

1. Introduction

Flames possess intrinsic instabilities associated with the combustion process itself. They could become unstable also in response to superimposed oscillations, among which pressure oscillations are the most common. The unsteady coupling between pressure oscillations and the flame leads to unstable combustion. This is the phenomenon of combustion instability. The suppression of this coupling is the essential mission of the control problem.

The strong coupling between pressure oscillations and the dynamics of unsteady heat release from flames arises in the following way. When a fluid element is heated during the combustion process, its expansion produces an initially weak pressure wave that radiates into the surrounding region. This pressure wave could get reflected from the boundary of the combustion system, and return to affect the flame surface slightly. This time-dependent effect results in a time-dependent volume change in fluid element in the combustion zone, and serves as a source of a new pressure disturbance. If the new disturbance is in phase with the old, a sustained feedback mechanism could lead to large amplitudes of pressure oscillations.

Large pressure oscillations limit the operating range of a combustion system by adversely affecting the stability and survival of the flame. They also produce intense vibrations, structural damage, and high burn rates. They may propagate upstream from the combustion zone and affect the composition of the fuel-air mixture; cause a change in the atomization and vaporization process in a system using liquid fuel; organize the unstable mode in the shear layer feeding the combustion zone; produce organized concentrated vortices through its interaction with geometrical discontinuities in the system, etc.

In February 1988, the *Wall Street Journal* ran the article, 'Turbine Makers Are Caught in Innovation Trap'. The article cited instances where new turbines of General Electric Corporation, Europe's GEC-Alsthom SA, Swiss-Swedish conglomerate Brown-Boveri, and Berlin's Siemens had to be shut down for reasons related to combustion instability. Thus, combustion instability continues to plague the industry and deserves attention. The understanding and control of combustion instability is important in a variety of systems such as liquid fuel rockets and ramjets. Combustion instability has also acquired increased urgency in recent years: for instance, lean mixtures are desirable for lower NO_x emissions (as mandated more and more by law) but some practical schemes for accomplishing this goal render the system more susceptible to combustion instability.

It must be noted that, while instabilities are a problem for continuous combustion systems, pulsed combustors can take advantage of oscillatory combustion.

2. Existing literature on the control of combustion instability

The literature on combustion instability is enormous and cannot be summarized adequately here. However, some representative sources are worth mentioning. Williams[2] provides an account of the basic theoretical understanding of instabilities and their amplification. This book cites 233 references at the end of the chapter on combustion instabilities. Two sections in the Twelfth Symposium (International) on Combustion[3] contain valuable articles on combustion instability by Crocco, Price, Marxman and Wooldridge, Sirignano, Zinn and Savell, Priem and Rice, Thring, Barrere and Williams, Kydd, Pariel and de Saint Martin, Beckstead, Mathes, Price and Culick, some of which are a pleasure to read even today. Similarly, the Thirteenth Symposium (International) on Combustion[4] dedicated two sections to

[†]For corresopondence. (e-mail: k.sreenivasan@yale.edu)
By his own contributions and through his enormous influence over generations of students and collaborators, Satish Dhawan has profoundly impacted the nature and quality of engineering science in India. It is a pleasure to dedicate this article to him.

oscillatory combustion, and contains articles by Zinn and Powell, Deckker and Sampath, Becker and Guenther, T'ien and Sirignano, Fletcher and Foley, Leyer and Manson, Sipowicz, Ryan and Baer, Ibberson, Beer, Swithenbank, Taylor and Thring. The book by Putnam[5] contains an excellent account of various ways in which the Rayleigh criterion, to be explained below in some detail, can be used to suppress combustion instability in industrial systems. The comprehensive volume on combustion instability in liquid rockets, edited by Harrje and Reardon[6], discusses feedback modeling scenarios for purposes of avoiding or rectifying the instability problem. Together, these sources provide the background on classical aspects of combustion instability and control.

In the Twentyfourth Symposium (International) on Combustion[7], the control of combustion instability reappears prominently after a lapse of some twenty years. In this volume, Candel particularly examines the coupling of combustion instabilities to fluid dynamics, and discusses various control strategies. The group of articles by Kemal and Bowman, Neumeier and Zinn, Davis and Samuelson, Laczak, Eisenberg, Knapp, Schlueter, Beushausen and Andersen, Hantschk, Hermann and Vortmeyer, Yu, Parr, Wilson, Schadow and Gutmark, Furlong, Baer and Hanson, Zimmermann, Lenior, Kettrup, Nagel and Boesl, and Leipertz, Obrtacke and Wintrich, collected in the Twentysixth Symposium (International) on Combustion[8], gives specialized perspectives on the modern understanding of active control of combustion instability. Adaptive control strategies, in which the system performance is monitored continually and the control parameters are controlled automatically to obtain good performance, form the core of the work of Annaswamy and Ghoniem[9]. These articles, along with the key references they cite, summarize much of the new information available on combustion instability and its control.

Combustion instability is a system-sensitive phenomenon. Although the source of pressure oscillations is the heat release from combustion, the properties of the oscillations are determined by the design and dimensions of the combustion systems. Thus, the causes of instability and the severity of its consequences, as well as the most fruitful control strategies to be adapted, vary from one system to another. A simple-minded classification of these strategies is in terms of passive or active schemes. Passive schemes are of the following type: (a) geometrical changes such as baffles aimed at suppressing the acoustic standing wave; (b) introduction of damping and dissipation through acoustic liners and Helmholtz resonators; (c) interference with the interaction between acoustics and combustion by the introduction of quater-wave tubes, etc. There are various versions of active control. For instance, one could extract energy from perturbations by cleverly deploying secondary energy sources that release heat out of phase with pressure fluctuations. This is largely the present approach. One could also use feedback methods based on some mathematical model of the dynamic behaviour of the flames. In this method, the stability of the model to small perturbation is examined, and the predicted stability limits are compared with experimental observations. Mathematical models allow one to study the stability of the system to finite disturbances, as well as to self-sustained oscillation resulting from the instability. Passive control schemes are easier to implement. Active control schemes are more desirable because they can satisfy complex performance criteria simultaneously. However, their feasibility is dependent on the availability of fast, accurate, inexpensive and reliable sensing and actuation devices.

A theoretical foundation for active control of combustion instability will be presented in §3. In §4, we shall discuss the control of pressure oscillations in acoustically-driven unstable system by heat addition. §5 and 6 describe, in much less detail, the control strategies based on injecting external forces and fluid mass. We shall demonstrate the effectiveness of the control techniques by considering a number of laboratory devices such as flame-driven longitudinal oscillations, organ pipe resonances, 'whistler nozzle', and vortex generation superimposed on broad-band turbulence. We shall also consider the instability in a combustion tunnel at the Aero Propulsion Laboratory, Wright Patterson Air Force Base, and suppress it. The paper ends with a summary and discussion in §7.

The work is abstracted from the Ph D thesis of Raghu[10], which should be consulted for more details. Two shorter summaries have previously appeared[11,12].

3. The fundamental equation for the active control of combustion instability

The conservation laws governing the motion and changes in a multicomponent fluid with chemical reactions can be written as:

$$\frac{\mathrm{d}\rho}{\mathrm{d}t} + \rho \nabla . \mathbf{v} = \dot{m} \tag{1}$$

$$\rho \frac{\mathrm{d}\mathbf{v}}{\mathrm{d}t} + \nabla p = \nabla . \mathbf{S} + \mathbf{F} \tag{2}$$

$$\rho \left(\frac{\mathrm{d}e}{\mathrm{d}t} + p \frac{\mathrm{d}}{\mathrm{d}t} (\rho^{-1}) \right) = \mathbf{S} : \nabla \mathbf{v} - \nabla . \mathbf{q} + \dot{Q} \tag{3}$$

$$\rho \frac{\mathrm{d}Y_i}{\mathrm{d}t} + \nabla . \mathbf{J}_i = w_i + \dot{M}_i, \quad i = 1,2,\ldots, N, \tag{4}$$

where $\mathbf{v}$, p, $\mathbf{S}$, $\mathbf{q}$, r, T and e denote, respectively, the velocity vector, the pressure, viscous stress tensor, heat

flux vector, the density, temperature and internal energy of the flowing fluid; Y_i and $\mathbf{J}_i$ are the mass fraction and diffusion flux of the 'i-th' one among the N species in the flow; w_i is the rate of production of species 'i' per unit volume of chemical reactions; d/dt stands for the material derivative, $(\partial/\partial t) + \mathbf{v}.\nabla$. The equations are standard when the source terms of mass $(\dot{m})$, momentum $(\mathbf{F})$, heat $(\dot{Q})$ and species $(\dot{M})$ are absent. By perturbing the medium slightly through the addition of a small body force, heat, mass, or species mass fractions, and manipulating the resulting equations, Chu[1] derived an equation for a positive definite quantity, E, that can be considered as a general fluctuation energy of the system. That is, this quantity vanishes when the perturbations to the system are zero and satisfies the familiar properties of energy. The equation can be written as

$$\frac{\partial E}{\partial t} + \nabla.\mathbf{J} = -\Phi + \sigma, \tag{5}$$

where $\mathbf{J}$ is the flux of the perturbed energy E, and Φ, also a positive definite quantity, is the dissipation rate of E, and the s term is responsible for pumping energy to the perturbation (when $s > 0$) or extracting energy from it (when $s < 0$). The equation is applicable to a multicomponent fluid medium, and not limited to an ideal gas behaviour or even to a Newtonian fluid; it is valid regardless of the transport laws assumed for heat and mass diffusion, or for reaction rate. When integrated over a region R enclosed by a control surface S, the above equation takes the form

$$\frac{\partial}{\partial t}\int_R E\mathrm{d}V + \int_S \mathbf{J}.\mathrm{d}\underline{A} = -\int_R \Phi\mathrm{d}V + \int_R \sigma\mathrm{d}V. \tag{6}$$

Here, the first term is the rate of increase of energy in the disturbance inside the region R and the second term is the rate at which the energy is radiated away from the region. The third term is the rate at which energy is dissipated by molecular action (viscosity, heat and mass diffusion as well as chemical reactions), and the last term represents the energy transfer to or from R by means of the addition of mass, heat or body forces, as well as additional species fluctuations. The interpretation of this equation is that, the energy of a disturbance in a system can be diminished or enhanced by working on s. (The dissipation term will always be positive definite and acts always to diminish the energy.) We shall therefore be concerned with the s term to develop our control strategies. The term has the following explicit form:

$$s = \frac{\dot{m}'p'}{r_0} + \mathbf{F}'.\mathbf{v}' + \frac{\dot{Q}'T'}{T_0} - \frac{T'}{T_0}\sum_{i=1}^{N} m_{i0}\dot{M}_i', \tag{7}$$

where r_0 and T_0 are undisturbed density and temperature, and m_{i0} is the undisturbed chemical potential of species 'i'. It is clear from eq. (6) that the perturbation energy within the system will decay if $\int_R s\ \mathrm{d}V$ is negative, and grow if that same quantity is positive and exceeds dissipation. Within a time interval corresponding to a perturbation cycle, the quantity of relevance is

$$\oint \mathrm{d}t \int s\ \mathrm{d}V. \tag{8}$$

The sign of this integral determines whether the perturbation grows or decays in time. The structure of s in eq. (7) suggests that one may render the integral negative by:

(a) periodic mass addition antiphase with pressure fluctuations;
(b) periodic body force antiphase with velocity fluctuations;
(c) periodic heat release rate antiphase with temperature fluctuations;
(d) species generation antiphase with the appropriate chemical potential.

It should be noted that temperature and pressure fluctuation are in phase with each other for the case of a purely acoustic disturbance. Then the energy can be extracted (see (c) above) from the disturbance by adding heat antiphase with pressure fluctuations, and energy can be added to a disturbance by adding heat in phase with the pressure fluctuation. This is the well-known Rayleigh criterion[13]. Rayleigh considered the case of thermally induced acoustic phenomena and noted: 'If heat be given to the air at the moment of greatest rarefaction, or be taken from it at the moment of greatest condensation, the vibration will be encouraged. On the other hand, if heat be given at the moment of greatest rarefaction, or abstracted at the moment of greatest condensation, the vibration is discouraged'. Rayleigh did not discuss the other means described above for increasing or decreasing the amplitude of the energy disturbance.

In the rest of the paper, we demonstrate that the ideas just outlined form the basis of control, at least in simple circumstances. Because of the limitations imposed by geometry and other operating conditions, there is no guarantee that these methods will always work in real systems; but the principles must apply to all combustion systems, though the question of how one approaches a particular problem depends on details. A study of several examples, which this paper attempts to do, will offer hints useful for any applied problem.

4. Control of pressure oscillations by heat addition

4.1 *Preliminary considerations*

We shall consider the simple case of the Rijke tube. This is a long tube with open ends, at one end of which sits a flame. Here, the tube is 125 cm long and 10 cm in diameter. An open flame from a burner of 2 cm diameter is inserted at about 10 cm from one end of the tube. See Figure 1. Almost immediately, a loud and nearly pure-tone noise can be heard. This noise is sustained and uncomfortably loud. It is this thermoacoustic mode that we shall suppress by suitable heat addition, taking guidance from the theory.

First, to understand the observed mode, let us recall from §3 that the rate at which energy is transferred to the acoustic mode due to heat addition is given by

$$\int \mathrm{d}^3 x \dot{Q}' T' / T_0(\mathbf{x}), \tag{9}$$

where $Q'(\mathbf{x}, t)$ and $T'(\mathbf{x}, t)$ are respectively the fluctuating components of heat release per unit volume and the temperature fluctuation, both at the location $\mathbf{x}$ and the instant t, $T_0(\mathbf{x})$ is the mean temperature at $\mathbf{x}$. The other terms in eq. (7) are zero here. The integration extends over the region where heat is being released. Whether or not a disturbance will be amplified depends on the sign of the integral of the above expression over a period of oscillation, namely

$$\oint \mathrm{d}t \int \mathrm{d}^3 \mathbf{x} \dot{Q}' T' / T_0(\mathbf{x}). \tag{10}$$

The implication of eqs (9) and (10) is that the condition most conducive for the growth of the disturbance is that the heat release rate fluctuation $\dot{Q}'$ and the temperature fluctuation T' must be in phase. As already noted, the temperature for the acoustic mode is in phase with the pressure fluctuation p', so that the controlling factor is the phase relation between $\dot{Q}'$ and p'. The condition for the growth or suppression of instability is

$$\oint \mathrm{d}t \int \mathrm{d}^3 \mathbf{x} \frac{\gamma - 1}{\gamma} \dot{Q}' p' / p_0(\mathbf{x}) > \text{ or } < 0. \tag{11}$$

The condition for suppression is sufficient because the dissipation also acts to suppress the oscillations.

Returning now to the system shown in Figure 1, when heat is imparted from the flame to surrounding air, two effects are produced. The heated fluid rises in the gravitational field, causing an upward draft through the pipe. The second effect is to produce a weak compression wave. This compression wave gets reflected from the open ends of the pipe. The boundary conditions constrain the pressure oscillation p' to assume a shape somewhat like that shown in Figure 2 *a*, oscillating back and forth with the maximum and the minimum occurring alternatively at the midsection of the pipe. (The presence of the flame makes this an approximate description, but does not change things qualitatively.) Associated with the fluctuating pressure is the fluctuating velocity superimposed on the mean draft. Corresponding to the instant when the midsection pressure is the least (as shown in Figure 2 *b*), the gas column is in the most rarefied state and the fluctuating velocity u' is everywhere zero (see dashed line in Figure 2 *c*). As the pressure in the tube starts to rise (for example, to a state shown by the dot-and-dashed line in Figure 2 *b*), the fluctuating velocity u' must be inwards both at the top and bottom ends of the pipe. The inward movement of air at the top is negative in the sign convention of Figure 2 *a*, while the inward movement of air at the bottom is positive. Hence, for the dot-and-dashed line in Figure 2 *c*, u' will increase from zero to a positive value at the lower end while decreasing from zero to a negative value at the upper end of the tube. The phase relationship between the velocity and pressure is then as follows: u' leads p' by $p/2$ in the lower half of the tube, and lags behind p' in the upper half. The same result could be seen mathematically as well. Neglecting losses, the equation governing the acoustic field can be written to a first approximation as

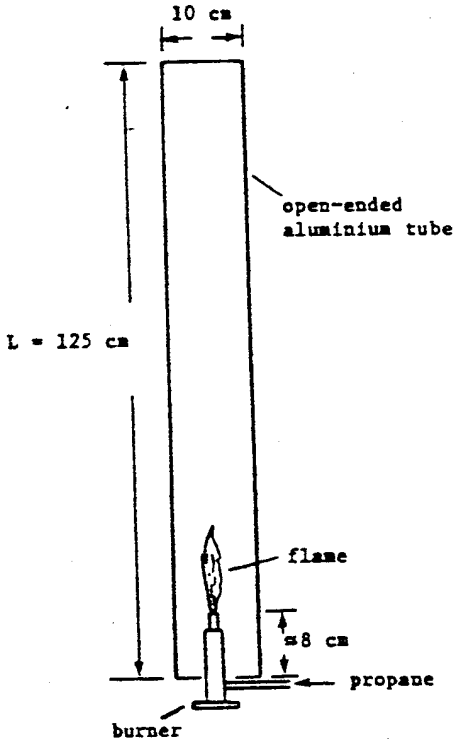

Figure 1. Schematic of the experimental apparatus.

$$\frac{\partial u'}{\partial t} = -\frac{1}{\rho_0}\frac{\partial p'}{\partial x}. \qquad (12)$$

If, say, $p' \sim \Sigma(x)e^{iwt}$, corresponding to the shape shown in Figure 2 *b*, it is easy to see from eq. (12) that

$$u' \sim \left|\frac{\partial \Sigma'}{\partial x}\right| e^{i(\omega t \pm \pi/2)},$$

where the prime denotes the derivative with respect to x, and the + and – signs hold respectively in the upper and lower halves of the tube. Thus, u' leads p' by $p/2$ in the lower half of the tube, while lagging behind by $p/2$ in the upper half. The pressure and velocity fluctuations

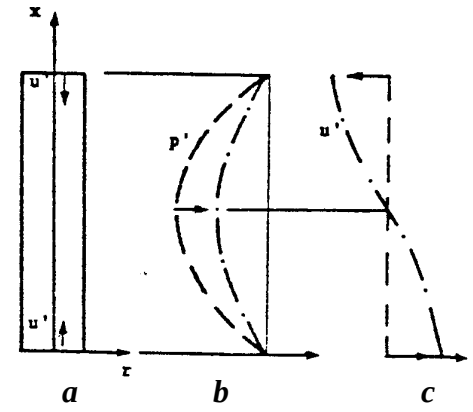

Figure 2. The pressure and velocity fluctuations in an environment of self-sustained oscillations.

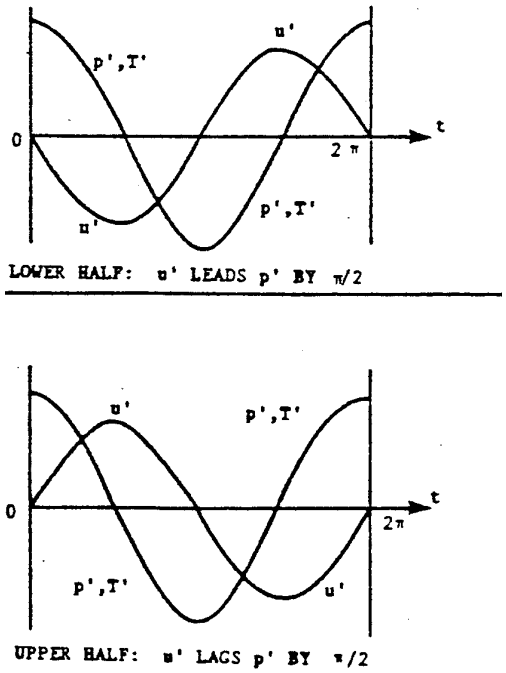

Figure 3. Schematic of variations with respect to time of velocity, pressure and temperature fluctuations at some typical positions in lower and upper parts of the pipe.

measured as a function of time at typical points in the lower and upper halves of the tube will look as shown in Figure 3.

Let us recall that our interest is in finding the phase relation between the temperature fluctuation and the heat release rate fluctuations. The velocity field affects the flame front and the extension of the flame sheet where combustion occurs. An upward fluctuating velocity will reinforce the mean draft, thus increasing the flame area and the rate of heat release. A downward velocity fluctuation produces the opposite effect. The precise phase lag between the fluctuating velocity and the fluctuating heat release cannot be deduced from qualitative arguments. In the absence of a full theory, one may resort to direct (and difficult) measurements of the heat release rate fluctuations.

One can also get a rough appreciation for the phase lag by replacing the burner in Figure 1 by an electrically maintained heating element where, too, the classical Rijke tone can be heard. Carrier[14] calculated the response to the environment of fluctuating flow field over the heater configuration of Figure 4: the heater was approximated by a series of parallel flat plates, each of which was placed in an infinite fluid medium. The principal result of his analysis is that the heat release rate fluctuation $\dot{Q}'$ lags u' by approximately $3p/8$. Combining this result with Figure 3, the overall situation is as shown in Figure 5. For the heater in the lower half of the tube, $\dot{Q}'T'$ is positive for most of the cycle so that its average over one cycle is substantially positive. If the heat source is sufficiently strong, the integral (11) exceeds the losses and self-sustained oscillations are set up. On the other hand, if the heater is located in the upper half of the pipe, u' lags p' by $p/2$ and so, keeping Carrier's result in mind, we can see that $\dot{Q}'T' < 0$ for the most of the cycle. The situation is thus stabilizing. It is this latter characteristic of the heater that suggests a method of controlling or suppressing the acoustic instability in a combustion system. To quench the oscillations in the system, it is only necessary to install a second heater – a 'control heater' – in the upper half of the tube. The attractive feature is that the control heater, even when supplied by a steady source, releases heat periodically with the right phase difference with respect to the pressure oscillations.

One may be inclined to think that for complete stabilization the power needed for the upper heater must be comparable to that required at the primary heat source. Simple considerations show that this is not so. In a steady-state periodic oscillation, the total energy supplied to the acoustic mode per cycle of oscillation must be equal to the total energy loss per cycle due to dissipation and acoustic radiation. But the acoustic energy accounts for only a small fraction of the energy of the primary heat source, a large part of which is spent in heating the oncoming gas.

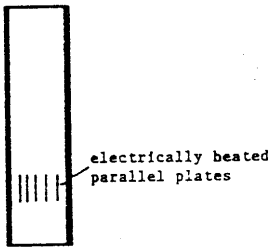

Figure 4. Schematic of configuration analysed by Carrier.

4.2 *Suppression of the Rijke tone*

We have verified that the Rijke tube oscillations can be suppressed indeed completely by placing a heater in the upper part of the tube. Even if the secondary heat source extracts only a small amount of acoustic energy per cycle, the amplitude of oscillation is bound to decrease with time. Of interest, then, is the dependence of the rate of decay of oscillations on the power needed at the control heater. The power required at the control heater depends on (a) the initial level of the oscillations and the percentage amplitude reduction sought, and (b) the time between the instant at which the control heater is turned on and that at which the stipulated level of reduction occurs – the so-called 'waiting time'. We shall now measure the waiting time for the case when the primary heat source and the control heater are both electrical. Both heaters are of similar construction and consist of a nichrome ribbon folded around a flat annular ring of asbestos. The solidity is approximately 40%. Estimates show that similar numbers are valid for flame-driven oscillations of Figure 1 quenched by the electrical control heater.

In Figure 6 are shown the ratio of power at the control heater to that supplied to the primary heater for a fixed waiting time (arbitrarily chosen to be 20 s). The data correspond to a crude heater design, and the power requirements were subsequently cut down by a factor of 10 by improving the control heater design. For these data, the primary heater is located at $L/4$ from the bottom, while the control heater is located at three positions L' from the top end, namely $L'/L = 0.25$, 0.17 and 0.13. The inset also shows, for $L'/L = 0.17$, the pressure oscillations for different values of the power ratio. We may note that the half-wavelength of these oscillations is equal to the pipe length, which indicates that the heaters do not significantly alter the flow and pressure oscillations. It is seen that the best position for the control heater, in terms of the least power needed, is $L'/L = 0.13$. The power ratio is of the order of 9% for a thousand-fold reduction in acoustic power. Figure 7 shows the power required for complete quenching as a function of waiting time. The power required is reduced to about a third if one is willing to wait 80 s instead of 10 s.

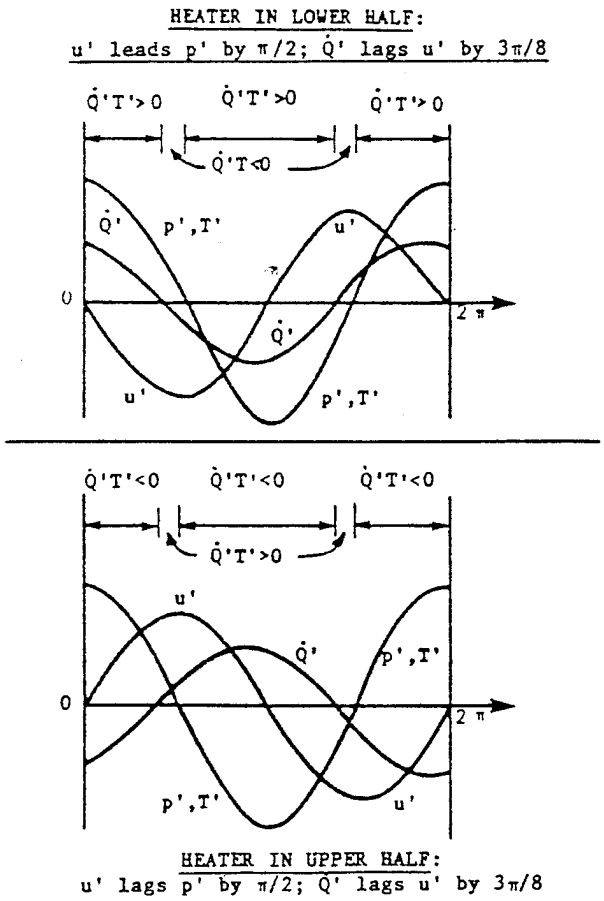

Figure 5. Phase relations between velocity, pressure (or temperature) and heat release rate fluctuations.

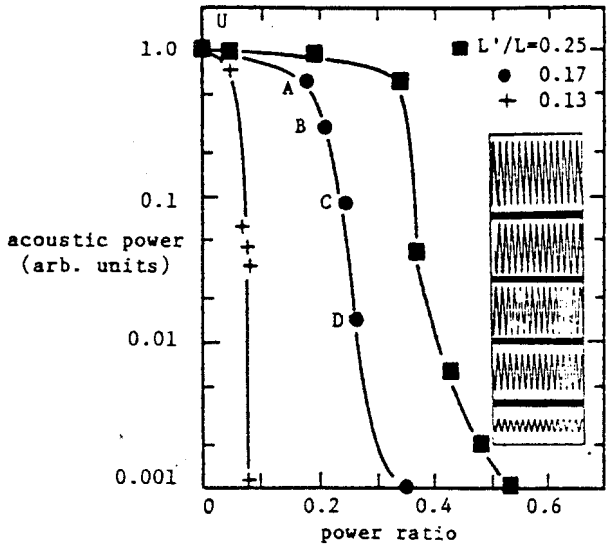

Figure 6. Reduction of the acoustic power attained as a function of the power ratio. Inset shows oscillograms (for $L'/L = 0.17$) of measured pressure fluctuations in the pipe. From top to bottom, they correspond respectively to U, A, B, C and D. The bottom three signals have a gain of 2 compared with the top two.

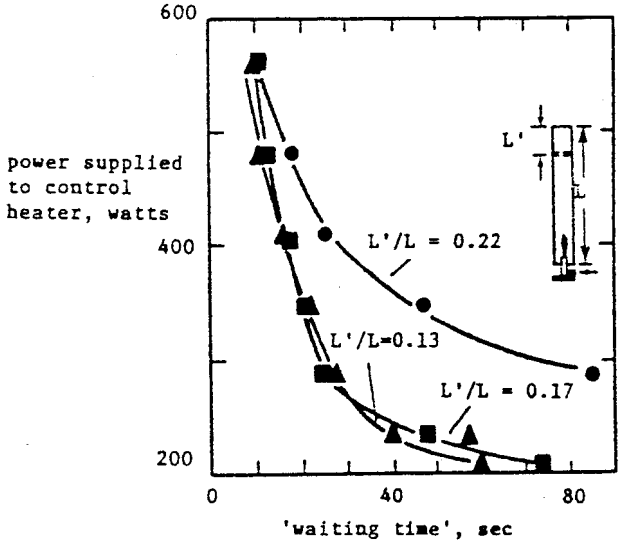

Figure 7. 'Waiting time' (that is, the time required for 'complete' quenching of oscillations) as a function of control heater power. Data are for flame-driven oscillations.

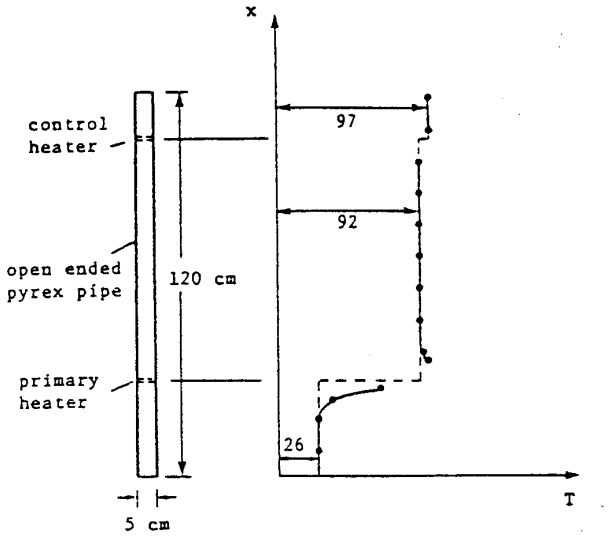

Figure 8. Measured temperature distributions (in °C) for a case of total control. Both heaters were maintained electrically. Dashed lines correspond to ideal distribution.

Table 1

Waiting time, sec	Power ratio	Additional temperature rise	Control heater power to acoustic power ratio
20	9%	7%	30
80	3%	2%	10

One consequence of the insertion of the control heater is the alteration of the temperature distribution of the original set up. Figure 8 shows a typical temperature distribution in the pipe when both heaters are electrically maintained. The temperature rises nearly discontinuously across both heaters, with the rise across the control heater being small compared with the overall rise. Dashed line represents the ideal distribution.

Table 1 provides some useful data on the power ratio as well as *additional* temperature rise in the presence of the control heater. For waiting times of the order of 80 s (for a particular set up), one pays the price of a 3% power and about 2% additional temperature rise for achieving total suppression of the acoustic oscillations. This power is still rather large compared with the acoustic power. Based on measurements from a calibrated microphone, we estimate that the acoustic power is only about 0.03% of the primary heater power, so that the control power required is more than an order of magnitude of the acoustic power. With the improved heater design, we can reduce the power requirement significantly.

4.3 *Suppression of the organ-pipe resonance set up by a loudspeaker*

Suppose now in the same vertical tube of Figure 1, we set up an acoustic resonance by tuning a loudspeaker so

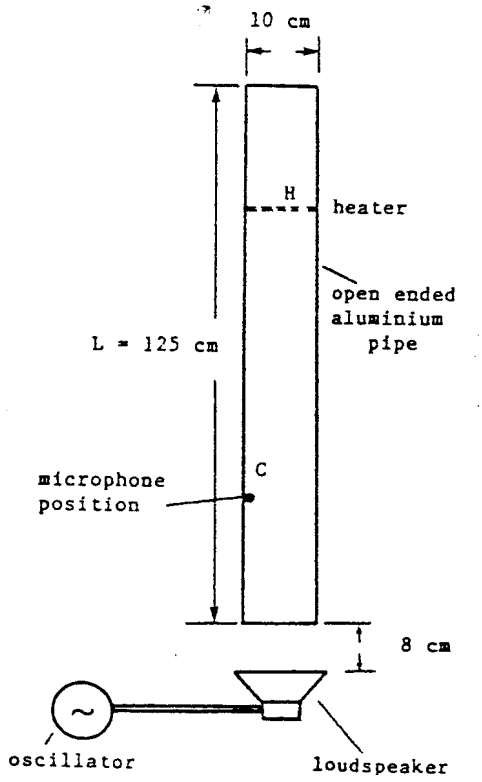

Figure 9. Schematic of set-up with loudspeaker-driven resonance oscillations. When the heater at *H* is turned on, the oscillations died out; see Figure 10.

that the half-wave length of the excited oscillation equals the pipe length (see Figure 9). Following the ideas of the previous sections, it would appear that the oscillation can be suppressed by placing a control heater somewhere in the upper half of the tube. Figure 10 shows the pressure signals with the heater (located at *H*) off as well as on. Clearly, the amplitude of the pressure oscillation drops off significantly in the presence of the heater.

The signals of Figure 10 were obtained by means of a condenser microphone mounted at the location *c* within the tube. The loudspeaker exciting the organ pipe mode is not strictly directional, and so the microphone will pick up the radiated signal from the loudspeaker, as a residual background from outside the tube, even when the oscillation within the pipe is completely suppressed. In fact, the oscillogram of Figure 10 *b* is very nearly equal in amplitude to the background level; so we surmise that the control heater has suppressed the resonance in the tube essentially completely.

Although the mechanism of suppression of resonance here is the same as that for the heater-driven case, an additional remark must be made. The flame as well as the heater set up a natural updraft, this being essential for introducing the proper phase relation between $\dot{Q}'$ and T' (or p'). Without the mean flow, the heat release rate from the heater will be merely a rectified sine wave, and can be considered to have two cycles for each cycle of the superimposed velocity fluctuation. It is the mean flow that sets up the required bias so that $\dot{Q}'$ follows u' with a phase lag. The control heater in the loudspeaker case will have to generate a mean draft in addition to releasing the fluctuating heat in proper phase. The process cannot therefore be as efficient in extracting energy from pressure oscillations as in the Rijke tube.

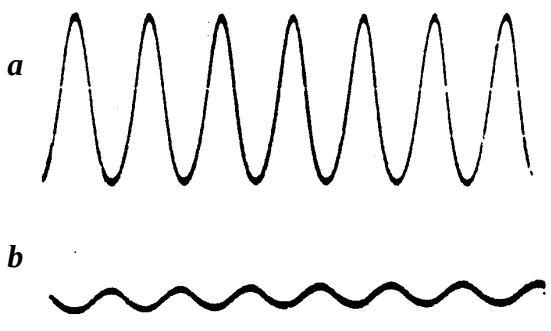

Figure 10. Pressure signals measured with a condenser microphone at C in Figure 9: (***a***) with the heater off, and (***b***) with the heater on. The signal measured with the heater on is comparable to the background level outside the tube.

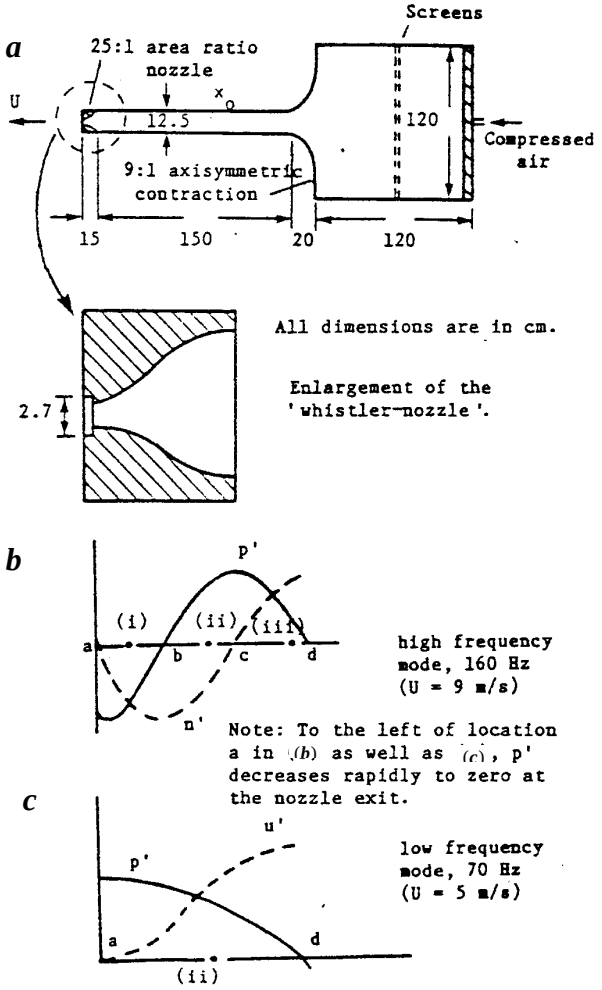

Figure 11. ***a***, The 'whistler-nozzle' apparatus; ***b*** and ***c*** are the *measured* mode shape of velocity and pressure oscillations. The location a in the Figures ***b*** and ***c*** corresponds roughly to the upstream end of the 25:1 nozzle.

4.4 *The control of the 'whistler nozzle' phenomenon*

As the next example, consider the whistler-nozzle phenomenon. Pressure oscillations here are set up by coupling the shear layer stability with the resonance of the chamber (see, for example, ref. 15). The present experimental arrangement, shown in Figure 11 *a*, consists of a 120 cm × 120 cm settling chamber contracting axisymmetrically to a 12.5 cm diameter pipe that is 150 cm long. This pipe will henceforth be called the 'test section'. To the other end of the test section is attached a fifth-order round nozzle of area ratio 25. Air flows through two screens, the settling chamber and the test section and exits through the nozzle. The nozzle has a small step, this being the crucial feature in establishing the audible whistler resonance. The mechanism is roughly as follows. When the shear layer develops a periodic velocity component by virtue of the most amplified mode, its impingement on the step produces periodic pressure oscillations. If the frequency of these oscillations matches one of the resonance modes of the chamber, a well-defined whistler resonance gets established. This, too, is audibly large.

The chamber of Figure 11 *a* resonates at two frequencies. The frequency is about 160 Hz for the flow velocity of 9 ms^{-1} (the 'high frequency' mode) and 70 Hz for 5 ms^{-1} (the 'low frequency mode'). The mode shapes are shown in Figure 11 *b* and *c*. Our objective is to control (suppress or amplify) these oscillations.

For the high frequency mode, the simultaneous measurement of the fluctuation pressure p' and the associated horizontal velocity fluctuation u' in the region a–b (Figure 12 *a*) and c–d (Figure 12 *b*) shows that u' leads p' by $\approx p/2$. Simple one-dimensional analysis of the flow ignoring nonlinearities and losses shows that this phase difference must be exactly $p/2$. The situation is analogous to the lower half of the Rijke tube. If a heat source of sufficient magnitude is located in this region, from analogy to Figure 5, it follows that the oscillations build up. On the other hand, in the region b–c (see Figure 12 *c*), u' lags p¢ by $\approx p$ /2, and the situation is analogous to that in the upper half of the Rijke tube. Again by analogy, it follows that a heat source located anywhere in the region b–c must stabilize the oscillations.

This is indeed what happens. Let us first consider suppression. Figure 13 *a* shows an oscillogram of pressure oscillations measured with a microphone located at some point in the test section; the heater itself is located at x_0 in the region b–c (see Figure 11), but is off. Figure 13 *b* shows that the power density of the signal peaks at about 160 Hz as expected and has a minor harmonic content. The background level is five or six orders of magnitude below the peak. When the heater is turned on, the microphone output is typically as shown in Figure 13 *c*, with the spectral density presented in Figure 13 *d*. The peak there has diminished by approximately five orders of magnitude and slightly above the background level. The background noise in the off-resonance condition and its power spectral density are shown in Figure 13 *e* and *f*, respectively. Clearly, when the heater is turned on, the signal levels are quite comparable to the background conditions of Figure 13 *e* and *f*. When the heater is moved to regions a–b and c–d, the oscillations are amplified, consistent with our understanding.

Now consider the low frequency mode of Figure 11 *c*. Figure 14 shows that, anywhere in the region a–d, u' leads p' by $\approx p/2$; this phase relationship is such that a heat source located in the region will enhance oscillations. For the typical position x_0 of the heater (see Figure 11 *c*), Figure 15 *a* and *b* show sample traces, with the heater off and on, respectively. Figure 15 *c* represents the power spectral density of the pressure signal with the heater off. To suppress the oscillations, it is necessary to locate the heater outside of the test section, perhaps upstream of the 9:1 contraction. For this practical reason, other methods of control may prove to be more useful here.

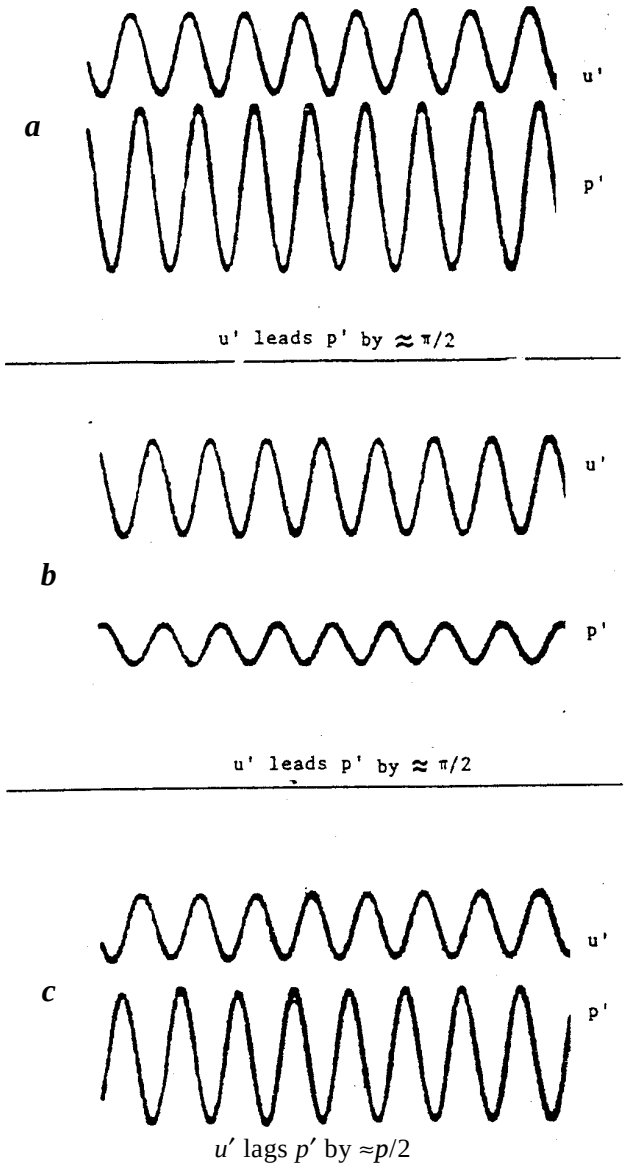

Figure 12. Velocity and pressure oscillations for the high frequency mode measured simultaneously in the test-section of the 'whistler-nozzle' apparatus of Figure 11. Signals in Figure 12 *a* were obtained at station (i) of Figure 11 *b*, while signals of 12 *b* were obtained at station (iii) of Figure 11 *b*. Heater anywhere in the regions a–b or c–d of Figure 11 *b* amplifies the pressure oscillations. Figure 12 *c* corresponds to measurements at (ii) of Figure 11 *b*. Heater anywhere in the region b–c of Figure 11 *b* suppresses oscillations; see Figure 13.

In all the instances of control discussed above, the pressure and velocity fluctuations are nearly periodic. The control was produced by controlling in the simplest way the phase between the heat release rate $\dot{Q}'$ and the pressure fluctuation p'. The problem reduces to making the integral of Putnam and Dennis[16], namely $\oint dt \int d^3x \dot{Q}' p'$, sufficiently negative. The present experiments are no doubt simple compared with real applications, whose many complexities might deny elegant

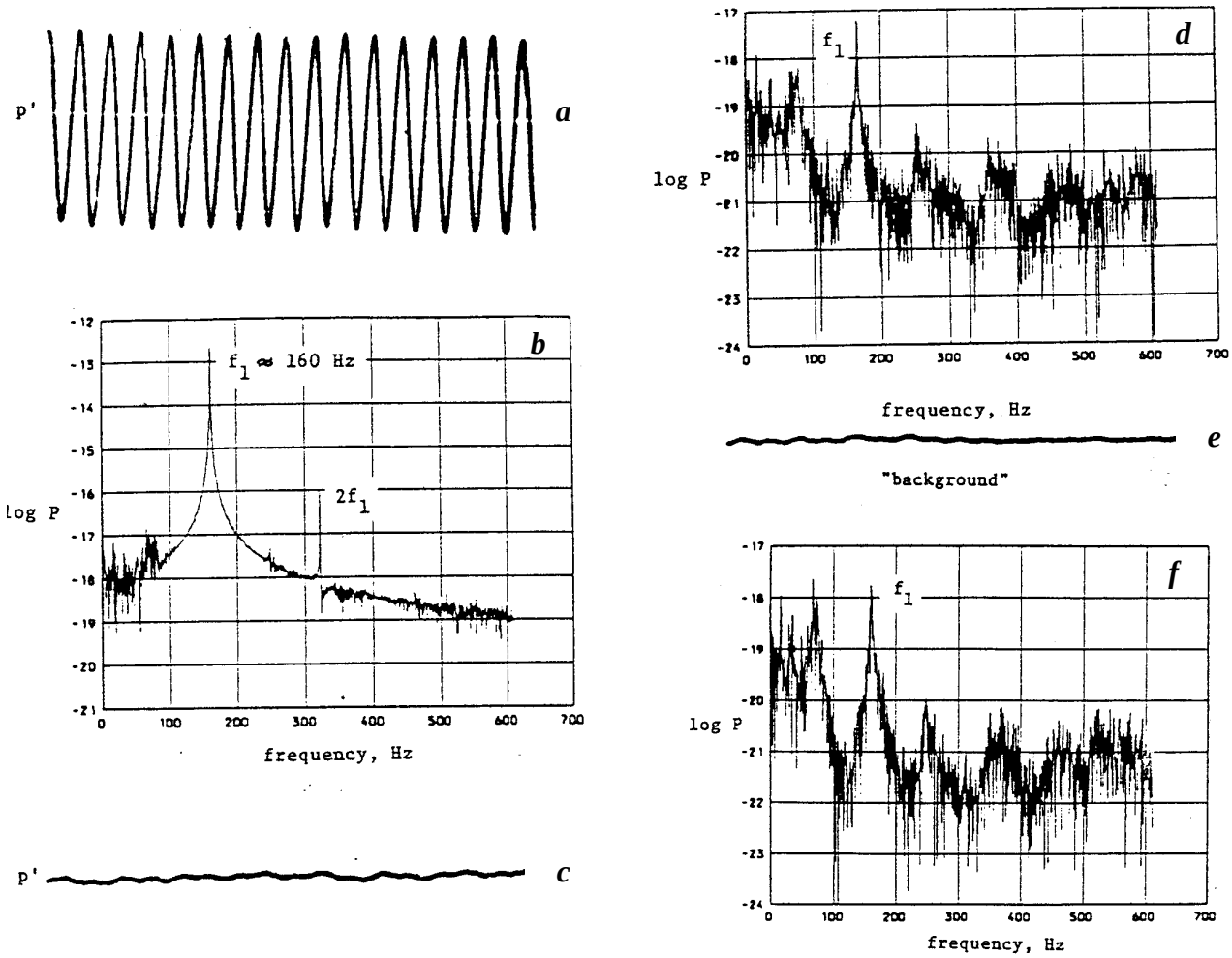

Figure 13. Oscillograms and spectral densities of pressure oscillations for the high frequency mode in the 'whistler nozzle' (***a***) and (***b***) correspond to no suppression, (***c***) and (***d***) correspond to suppression with heater located at x_0 in Figure 11 (***a***); (***e***) and (***f***) are background fluctuation levels.

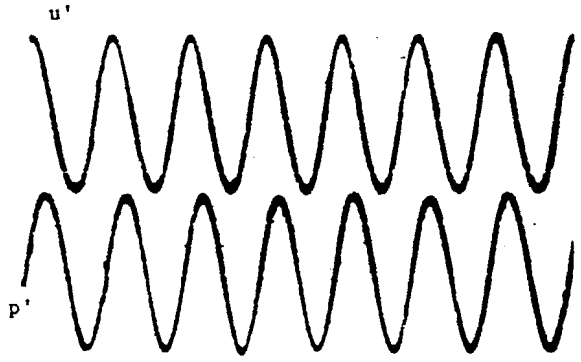

Figure 14. Velocity and pressure oscillations in the 'whistler-nozzle' for the low frequency mode. Measurements correspond to the station (ii) of Figure 11 *c*. Note that u' leads p' by $\approx p/2$. Thus, heater located anywhere in the region a–d of Figure 11 *c* leads to amplification of oscillations; see Figure 15.

solutions. Among other things, real systems are turbulent and involve quite high temperatures. We shall not say anything about the latter factor but demonstrate in §4.5 that these same ideas work even when turbulence is superimposed on periodic pressure oscillations.

4.5 *The control of pressure oscillations by heat addition in a turbulent pipe flow*

We examine in this section the control of acoustic standing waves generated in a turbulent pipe flow by the coupling of a shear layer instability with the organ pipe resonance of the system. The experimental system (Figure 16) consists of a pipe 185 cm long, 7 cm diameter, in which an annular ring of 3.3 cm diameter is positioned 5 cm from the upstream end. The upstream end is connected to a 9:1 contraction nozzle which in turn is connected to a large plenum chamber supplied with air from a centrifugal blower. Pressure oscillations were measured by means of a condenser microphone and velocity signals by means of a hot-wire operated on a con-

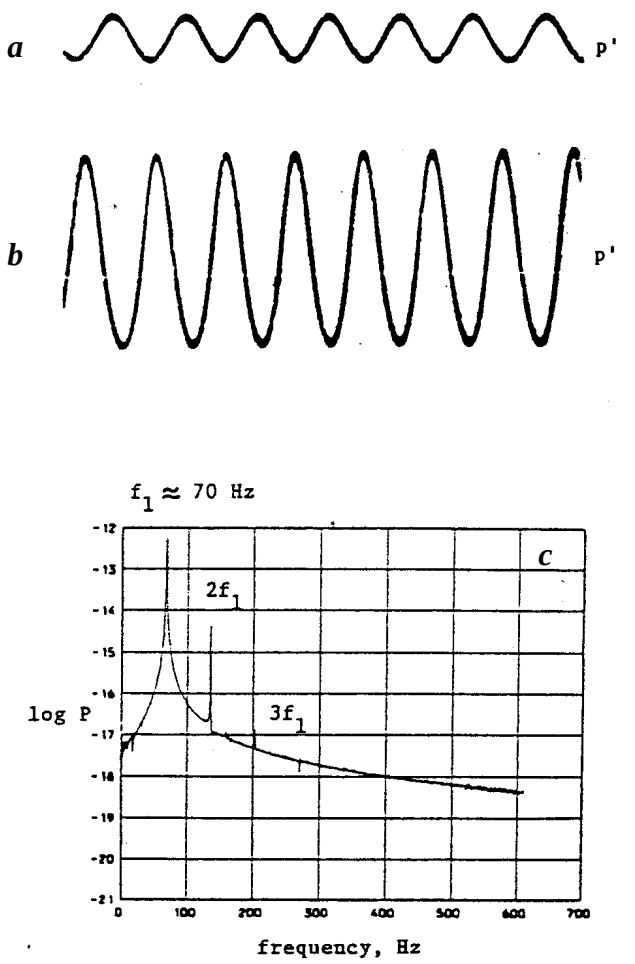

Figure 15. Amplification of pressure oscillation for the low frequency mode in the 'whistler nozzle' when the heater is located at x_0 in Figure 11 *a*. Figure 15 *a* is obtained with heater off, 15 *b* with heater on; 15 *c* is the power spectral density of the signal shown in Figure 15 *a*.

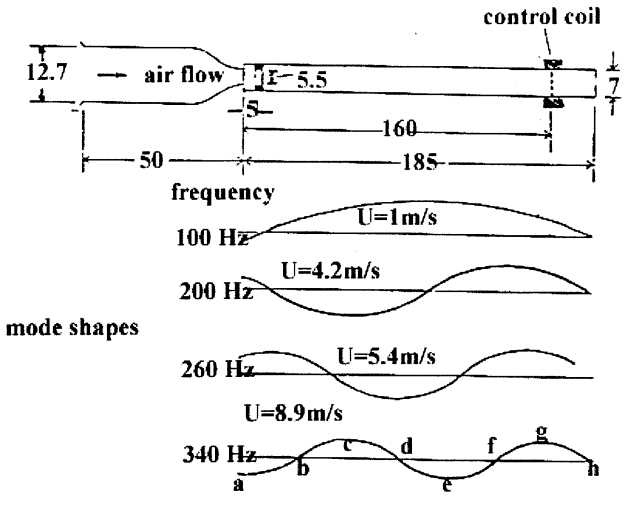

Figure 16. Schematic of experimental apparatus. All dimensions are in centimeters.

stant temperature anemometer (DISA 55M01). Mean velocity was measured at the pipe exit by a Pitot tube connected to a pressure transducer.

Four pressure modes could be established in this arrangement, depending on the flow velocity. Table 2 shows the frequency of each mode and the centerline flow velocity at which it occurs. These modes arise from the nonlinear interaction between the natural instability of the shear layer and the resonant modes of the pipe. Stronger the feedback, the more organized is the roll-up of the shear layer and the stronger the standing wave.

The mode shapes (Figure 16) were measured by traversing the microphone from end to end. Because of the inherent limitations of the experimental arrangement (e.g. poor heat resistivity of the pipe and the design of the collar housing the heating coil – see later), the major part of the experiments was confined to modes II, III and IV.

Figure 17 shows a typical velocity trace of mode IV (chosen for illustrative purposes). It has no discrete peaks, as shown by the power spectral density. Figure 18 shows that the pressure oscillations, on the other hand, possess spectrally discrete oscillations. Power spectral density shows that there is a strong peak around 340 Hz, and a weaker one at 200 Hz. Both velocity and

Table 2

Mode number	I	II	III	IV
Frequency, Hz	100	200	260	340
Velocity, cm/s	100	420	540	890

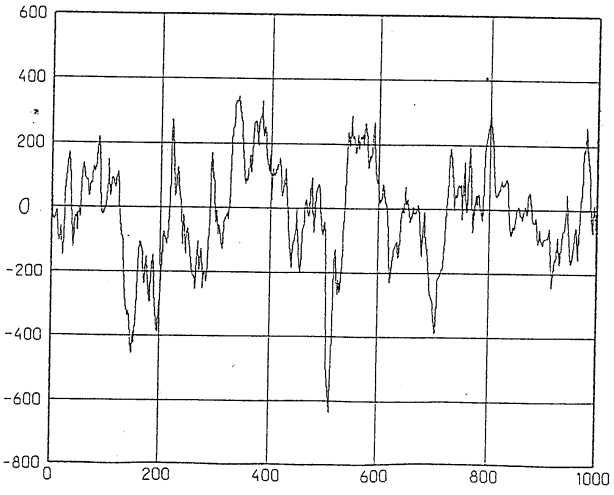

Figure 17. A time trace of the streamwise velocity flotation u' in the pipe. Units for the ordinate are arbitrary; for the abscissa, 100 units equal 0.01 s.

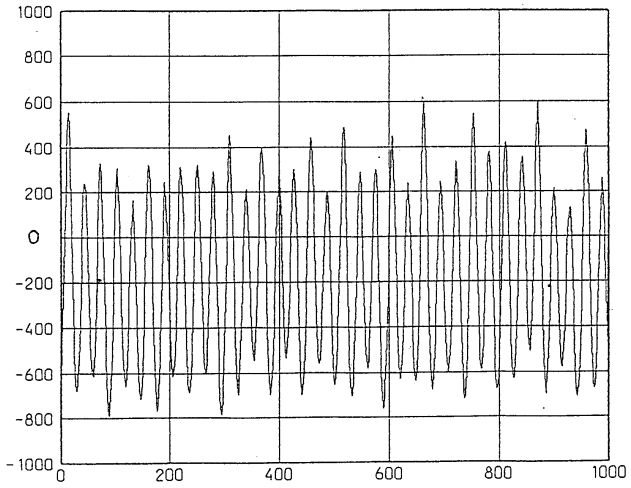

Figure 18. A time trace of the pressure fluctuation p' in the pipe. Units for the ordinate are arbitrary; for the abscissa, 100 units equal 0.01 s.

pressure signals were obtained at $x = 104$ cm. The potential reduction in pressure oscillations depends on whether there is a periodic heat release sufficiently out of phase with them. In the examples of §4, periodic heat release from a steady heat source was possible essentially because the mean flow velocity contained *periodic* fluctuations. Since the velocity fluctuations in the present instance are broadband, it is not clear if the same mechanism will work. One may hope to attain some degree of control if there is a coherence between the dominant pressure mode and the appropriate spectral component of velocity fluctuations. One further uncertainty concerns the location of the control heater because one cannot, in general be guided here by the type of considerations of §4. The use of band-pass velocity, with the center frequency corresponding to the periodic component in the pressure, does not help in practice. Even so, taking guidance from the non-turbulent case, it might be thought that locating the heater at 80 cm and 160 cm should have the opposite effects for mode III (260 Hz), while it would have like effects for modes II and IV. We limit ourselves to checking this issue below.

Keeping constant the electrical power input to the heater, we obtained the ratio of the mean square pressure with and without the control heater. Table 3 shows that there is generally a substantial reduction of the mean square energy when the heater is located at 80 cm, except for mode II for which it is only marginally effective. The 160 cm position, on the other hand, produces an attenuation of modes II and IV, and a reinforcement of mode III, as expected. The mean-square velocity fluctuation showed no perceptible change for any combination of conditions though the component filtered at the appropriate mode frequency showed a reduction of the order of a few per cent. Figure 19 is a time trace of

Table 3

Mode	II		III		IV	
x, cm	80	160	80	160	80	160
Acoustic power ratio	0.96	0.55	0.16	1.5	0.4	0.61

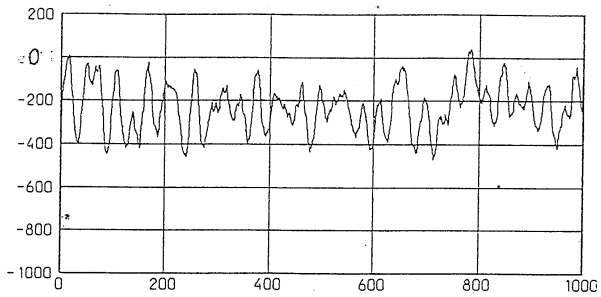

Figure 19. A time trace of the pressure fluctuation after control. The ordinate and abscissa are plotted to the same scale as in Figure 18.

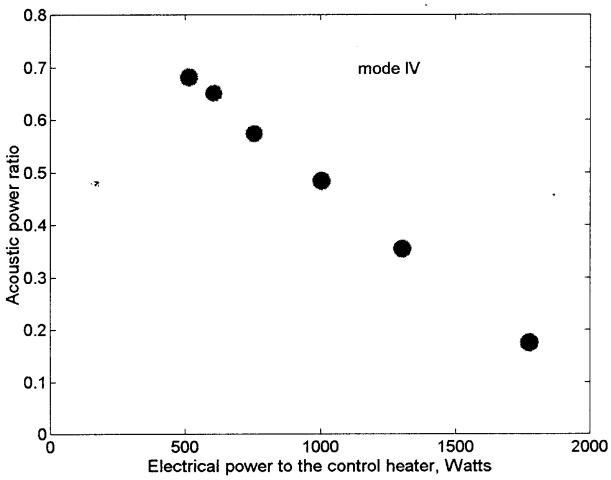

Figure 20. Power ratio for the control heater at 160 cm in the pipe.

the pressure mode IV, with the control heater in place. Figure 20 shows the acoustic power ratio as a function of the heating power supplied to the coil. It is clear that over a range of heating conditions, the degree of control depends directly on the amount of heating.

A complete understanding of the turbulent case is not possible because of the complex nature of the flow field. The likely reason for the partial success just described is the possible existence of a relatively strong cross-spectral correlation between the pressure and velocity fluctuations at the frequency of the pressure mode. We measured the cross-spectral correlation between p' and u', and found that there was indeed a strong correlation. With control, the correlation at 340 Hz became weaker though that at 200 Hz remained essentially unchanged.

5. The method of force addition

5.1 *General remarks*

The goal here is to suppress pressure oscillations by periodic injection of body forces such that the energy transfer by the momentum source, namely, $\int d^3x \mathbf{F}'.\mathbf{v}' < 0$ (the second term in eq. (7)). Here, $\mathbf{F}'$ is the fluctuating external force added to the fluid volume and $\mathbf{v}'$ is the velocity fluctuation in the system. External sources can be generated in different ways – centrifugal forces, magnetic forces, drag forces, etc. – but we confine our discussion to the drag force because it is the simplest to generate. Consider a cylinder in a fluid flow. When a fluctuating velocity is one-dimensional and varies, say, as $u' = u_0 \exp(iwt)$, then the drag force can be written as $D \exp(iwt + f)$, the phase angle f being a function of the velocity and the frequency of oscillation. Up to Reynolds numbers of the order 1000, the phase differences are such that the integral $\int d^3x\, \mathbf{F}'.\mathbf{v}' < 0$; that is, the drag vector is opposed to the velocity vector[17].

Consider placing a fine screen in a system in which finite pressure oscillations are superimposed on a flow. The screen generates a body force, which has steady as well as fluctuating components. The steady component does not contribute to the suppression of oscillations because the integral $\int d^3x \mathbf{F}'.\mathbf{v}' = 0$. The important effect comes from the unsteady part. If the Reynolds number, *Re*, based on the diameter of the screen wire is small, the drag coefficient, C_d, can be approximated reasonably well by $C_d \propto 1/Re$. If the screen can be approximated by cylinders, the total drag depends on the cumulative length of the wire in the screen. Hence, the drag of the screen will be proportional to its solidity. A solid disc of the same solidity does not, of course, produce the desired effect: it would alter both flow and acoustic fields.

5.2 *The whistler nozzle*

We use fluctuating drag force to control pressure oscillations in the whistler nozzle described in §4, and study mode II. Three screens were used (see Table 4). The maximum Reynolds number based on the screen wire was about 9. For all conditions, the drag was measured to be nearly out of phase with the the flow velocity.

Table 4

Screen	Solidity	Mesh, cm	Wire diameter, cm
1	0.4	0.32	0.68
2	0.5	0.16	0.38
3	0.6	0.08	0.31

Hence the value of the integral $\mathbf{F}'.\mathbf{v}'$ over a cycle was always negative and energy was extracted from pressure oscillations in the pipe, the exact amount being proportional to $\mathbf{F}'$. The screens were mounted on a thin annular plexiglass ring which was placed either at velocity nodes or at antinodes. In our experiments, for mode II, antinodes are present at $x = 70$ cm and $x = 160$ cm, and nodes at $x = 19$ cm and $x = 115$ cm. The microphone was always placed at a distance of 37 cm (chosen arbitrarily) upstream from the nozzle exit. Figure 21 shows some typical results when the screen was at the pressure node.

To increase the effectiveness of this method of suppressing pressure oscillations, it is necessary to increase the fluctuating component. This can be accomplished by oscillating the screen. The screen was oscillated antiphase with the velocity fluctuations by a feedback system. The pressure fluctuations were sensed by a microphone, and their phase was shifted before using them to drive the oscillating screen. The advantage of oscillating screens is that arbitrary phase difference can be established between the drag and the velocity fluctuation at the screen. This makes it possible to reduce pressure oscillations by mounting the screen at *any* convenient place in the system. See Figure 22 for results

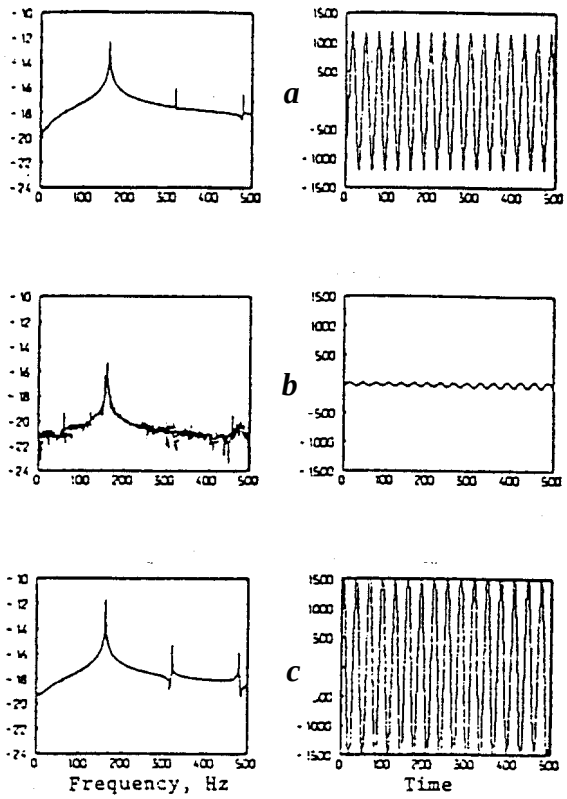

Figure 21. Power spectrum and time traces of pressure signals in the whistler nozzle for (***a***) no control, (***b***) suppression and (***c***) amplification. Screen located at $x = 70$ cm.

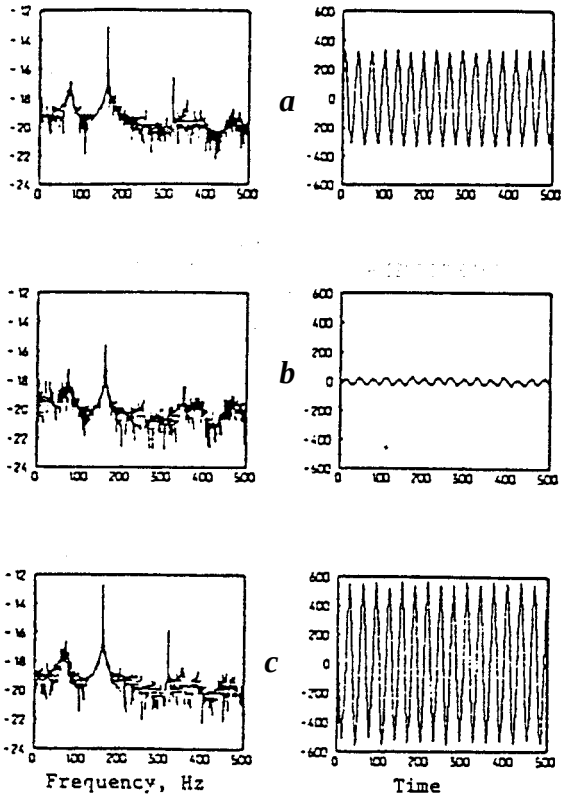

Figure 22. Power spectrum and time traces of pressure signals in the whistler nozzle for (***a***) no control, (***b***) suppression and (***c***) amplification. Screen located at x = 19 cm.

when the screen was placed at the velocity node. This result is important because, in practice, the pressure nodes may not always be accessible in practice.

Thus, in summary, periodic force addition (drag force in our case) can be used to control pressure oscillations. A stationary screen must be positioned at the velocity antinode to produce the best effect. Within the range covered, higher solidity of the screen produced greater reduction in amplitude. However, we have to pay the penalty of higher drag for screens of larger solidity. If the screen can be oscillated at a suitable phase with respect to velocity fluctuation at the screen, pressure oscillations can be reduced by positioning the screen *anywhere* in the system.

5.3 *Organ-pipe modes in a combustion tunnel*

In this section we describe the suppression of the organ-pipe mode in a combustion tunnel at the Wright Patterson Air Force Base, Ohio. A schematic of the facility is shown in Figure 23. See ref. 18 for details. Briefly, a 2.5 gal/h, 60 degree spray angle nozzle was used to inject the liquid JP-4 into a swirling air flow. The primary swirl air flow was maintained constant. The characteristics of the acoustic oscillations in the tunnel are governed by the length of the tail pipe from the burner. This is about 5.3 m long, resulting in the dominant oscillation at a frequency of about 100 Hz. The mode shape determined by traversing a microphone is also shown in Figure 23.

The acoustic level was quite high (of the order of 120 dB) and could not be suppressed by the application singly of either strategy discussed above. Thus, both heat addition and force addition were used in conjunction. Two 80-mesh screens of solidity about 70% were positioned at the velocity antinodes (where the velocity fluctuations are the largest). Four commercially available heating coils (20 cm diameter and 2300 W) were positioned near x = 290 cm. The position corresponds to the location where heat addition discourages pressure oscillations. A thin steel wire screen of 45 mesh was sandwiched between each pair of heating coils to have uniform heat release in the whole cross-section of the tunnel.

Without control, the sound level measured on the tunnel wall was about 116 dB (see Figure 24 *a*). Spectral peaks occurred at the resonance frequency and several of its harmonics (Figure 24 *b*). High speed movies of the flame indicated a highly organized vortex motion in the flame, with the large pressure oscillations producing periodically shed vortices from the lip of the burner shroud. This causes a periodic variation in the flame front, thus releasing heat also with a periodic variation. Independent luminosity measurements confirmed this picture. With control, the acoustic level improved by between 10 and 20 dB, as shown in Figure 24 *a*, and the spectral peaks diminished significantly (Figure 24 *c*). Even when the oscillations did not die away completely, at least a 10 dB reduction was possible. High speed motion pictures showed that the strongly organized vortex motion was significantly reduced. The operating boundary was extended significantly by the control method (Figure 25). Further details can be found in ref. 10.

6. Control by periodic mass addition

The relevant integral associated with control by mass addition is

$$\oint \mathrm{d}t \int \mathrm{d}^3x \dot{m}' p', \tag{13}$$

related to the first term in eq. (7). Fluctuations decay in time if this integral is negative. Periodic mass sources can be generated by applying periodic pressure gradient in a pipe or channel flow, or by periodically evaporating liquid droplets, or by periodically varying the exit area at the end of a secondary mass flow source, and so forth. We have made preliminary calculations on the effectiveness of evaporating liquid fuel to obtain peri-

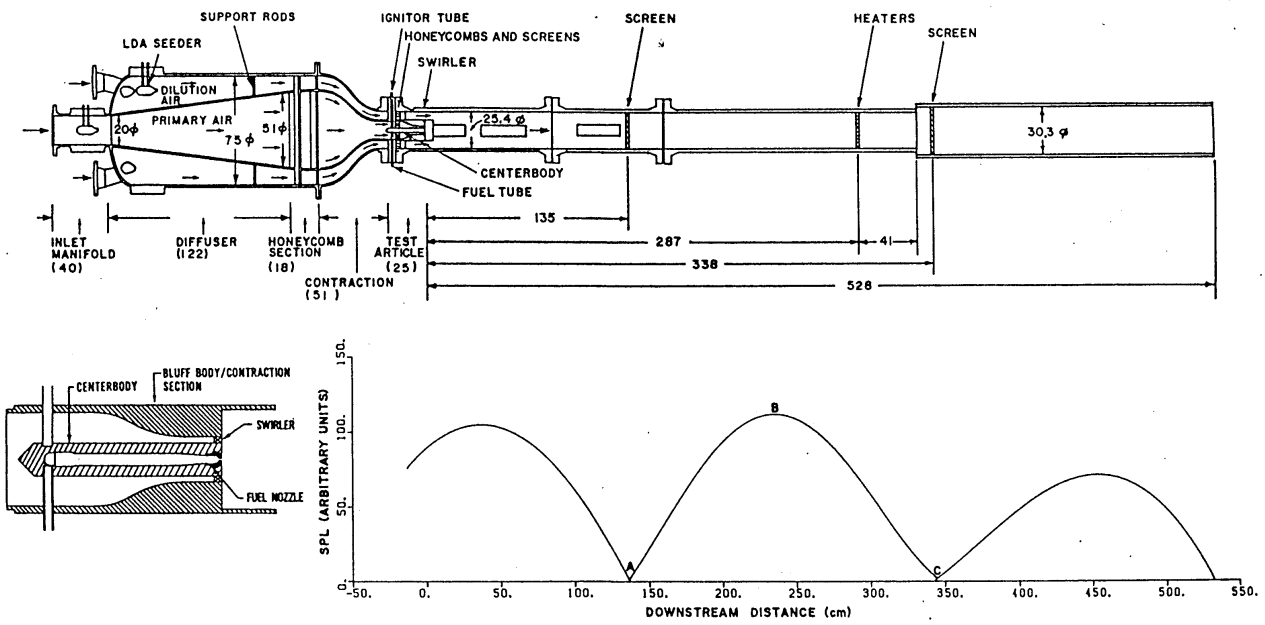

Figure 23. The combustion tunnel facility and the mode shape for the fundamental resonance frequency. Dimensions in centimeters.

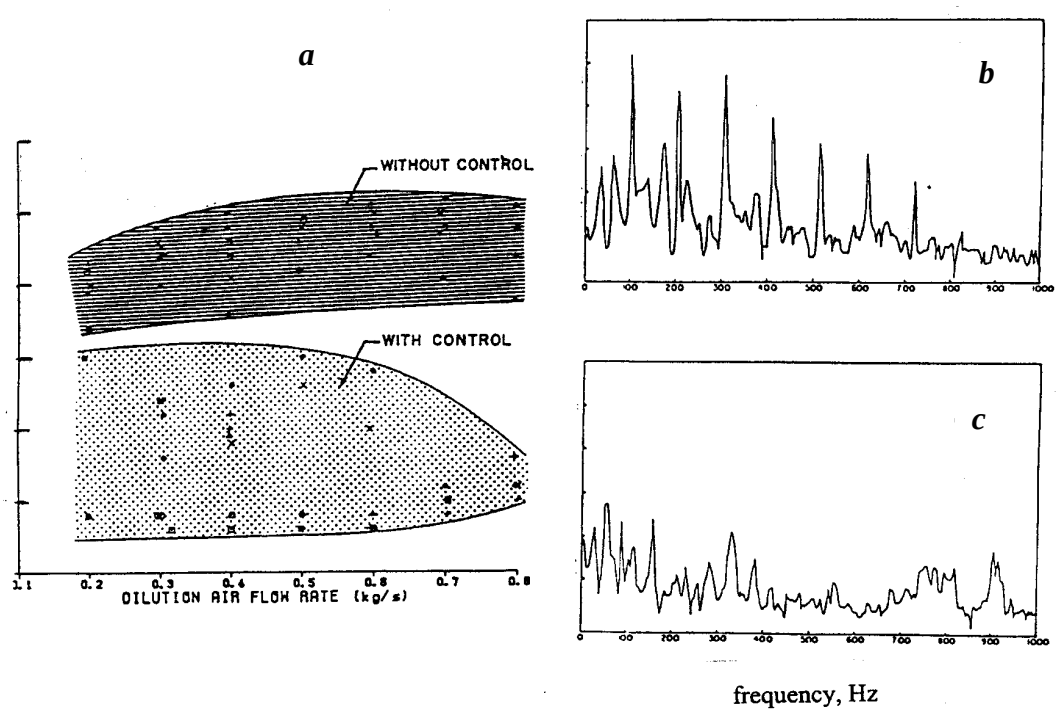

Figure 24. The sound pressure level with and without control. ***a***, Regions of operation with and without control. The ordinate is in decibels, with each mark measuring 5 dB, the top-most mark being 120 dB. (***b***) and (***c***) are, respectively, the spectral densities of pressure at typical points in the hatched and dotted regions in (***a***). The ordinates are in logarithmic units, and each mark represents 10 dB in power.

odic mass injection but have not attempted the scheme in a real experiment. Instead, we have used the variable area method. In the Rijke tube and whistler nozzle arrangements, the oscillations are quite sensitive to the mass flow rate, so they did not seem to be robust test cases for study. The case that seemed robust was one in which pressure fluctuations were established by driving a sound source at its resonant frequency (see §4.3). The loudspeaker was maintained at one end of the tube, while the periodic mass source was positioned at the other end. The mass source consisted of air flowing from a compressor tank. The flow rate was modulated through a slit whose area could be controlled periodically. Pressure signals were measured by a microphone placed at the middle of the tube.

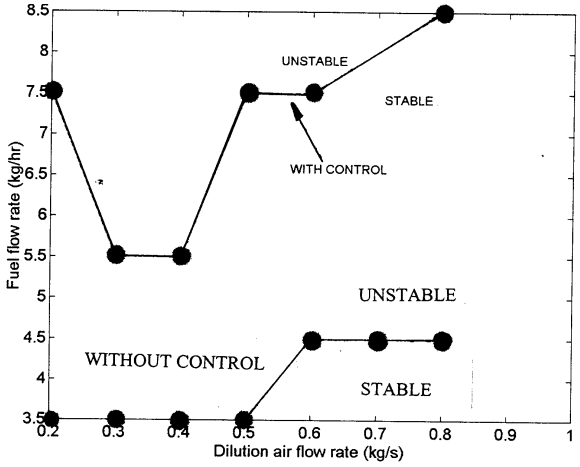

Figure 25. Stability margin of the tunnel with and without control.

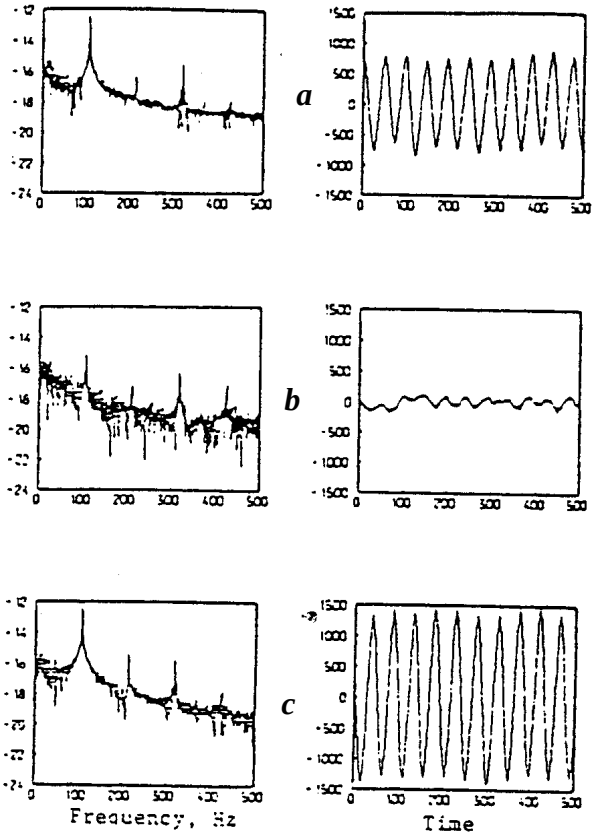

Figure 26. Pressure signals in the pipe during control by direct method. ***a***, No control; ***b***, Suppression and ***c***, Amplification.

The area of the slit was varied by oscillating two sharp blades in opposite directions. To determine the phase relation between the input voltage and the displacement of the blades, we studied the response of that system first. The response of control devices to imposed inputs is in fact an integral part of all control schemes. Control was effected in two different ways. In the first method, the same signal source was used to drive the loudspeaker and the blades forming the variable area slit. The phase of the signal supplied to the oscillating blade was shifted until the oscillations were completely suppressed (compare Figure 26 *a* with *b*). A constant amount of energy is expended in each cycle because of the mass addition to the system, and hence the control is of the open loop type. When the signal to the blades were inverted with respect to the case of suppression, the oscillations were amplified (compare Figure 26 *a* with *c*). The method is similar to that used by Strykowksi and Sreenivasan[19] for the suppression of Tollmien-Schlichting waves. The second method involved feedback to the pressure oscillations. This method was equally effective for both suppression and enhancement (see Figure 27 *a–c*). The particular feedback method used here suffers from the fact that the blades do not oscillate, because of inertia, when the amplitude of pressure oscillations falls below a threshold value. Hence, in this method of control, fluctuations of a certain amplitude always remain. This residual amplitude can be decreased by increasing the sensitivity of the mass addition system.

7. Summary and discussion

We have shown that control of acoustic oscillations can be achieved in a number of systems. The approach is

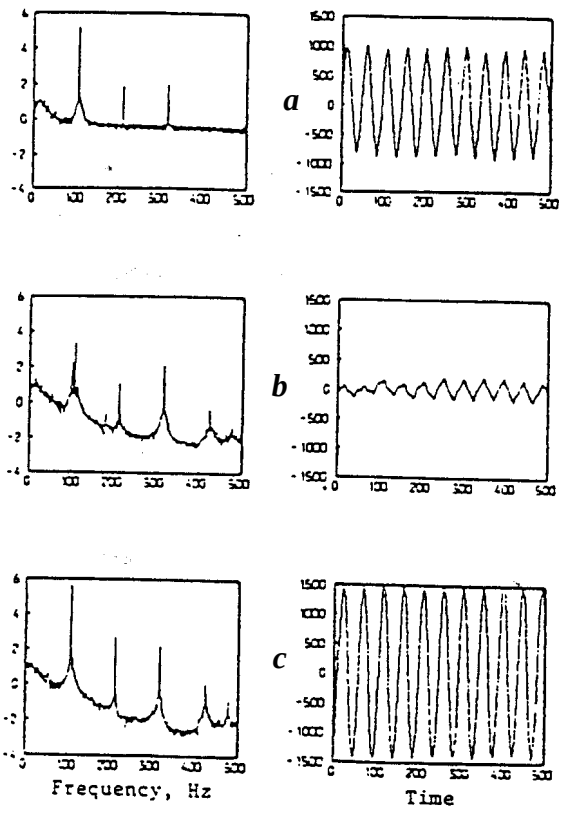

Figure 27. Pressure signals in the pipe during control by feedback method. ***a***, No control, ***b***, Suppression and ***c***, Amplification.

based on the concept of active control of acoustic oscillations which sustain the instability. By active control, we mean a method which attains the desired end – namely, the control of acoustic feedback sustaining the combustion instability – by extracting energy from the perturbations. The viability of the approach was demonstrated by several simple examples.

The basic result derived from the theory is an equation governing the 'energy' in a disturbance, namely eq. (6). The theory indicates that three distinct types of active control are possible: through a system of imposed body forces, or sources of mass and heat. Any one of them, or a suitable combination of them, can be used to control the pressure fluctuations in a system. The control device will have to be placed at such locations that render the integral

$$\oint \mathrm{d}t \int \sigma \mathrm{d}V < 0, \tag{14}$$

where the structure of s is displayed in eq. (7). This is a generalization of the Rayleigh criterion for acoustic disturbances.

We have successfully used these ideas to control acoustic oscillations in a number of laboratory systems. Our experience with the heater device used here indicates that the technique possesses two special qualities: (1) selectivity or specificity – that is, its ability to suppress selectively one or the other acoustic mode by properly positioning the devices, and (2) insensitivity – that is, its action is not very sensitive to the exact location within the device. These qualities are shared by the other two methods of active control as well.

Future efforts on active control, within the present philosophy, could proceed in several directions. In the development of other effective and adaptable devices, the response to acoustic oscillations should be analysed both theoretically and experimentally. This applies to 'volume' devices which aim towards yielding large negative values of s as well as to 'surface' devices which aim to yield large positive contributions to the term $\mathbf{J}.\mathrm{d}\mathbf{A}$ in eq. (6).

The feature which complicates the control of combustion instability is that the phenomenon is system-sensitive. This difficulty may be circumvented to some extent by examining the response of each component part of the system to an acoustic disturbance. The framework established here will then help us isolate the particular process in a system that is responsible for pumping energy into the disturbance. Focusing attention on a part of a system allows one to simplify the modeling as well experimental exploration.

An important point to bear in mind is that the response characteristics of the control device need to be known in order to implement the desired control effect. Mechanical devices have drawbacks at higher frequencies, and so one may turn attention to optical methods which produce similar effects. For instance, periodic mass injection may be attained by periodically evaporating liquid fuel droplets using a pulsed laser.

The present work has dealt with only longitudinal modes of oscillations. Transverse and azimuthal modes of instability are also known to occur in combustion chambers. The same method of control should be possible in principle even for these modes. The problem arises only when the standing wave is not stationary but oscillates randomly around a mean position (as has been observed in some instances of ramjet instability). From our present results, we have seen that the control is insensitive to a wide range of positions of the control device as long as the phase difference between the control heater and the pressure oscillations is less than 90 deg. Small changes in phase should therefore not matter though the relative efficiency of a particular scheme will depend on it. Our methods of control should be good for propagating waves as well, though there is the difficulty of tracking the phase of a propagating wave. A main point to emphasize is that the present techniques apply for finite amplitude disturbances, unlike classical wave cancellation techniques.

1. Chu, B.-T., *Acta Mechanica*, 1965, **1**, 215.
2. Williams, F. W., *Combustion Theory*, Benjamin Cummings, Menlo Park, CA, 1984, second edn.
3. Twelfth Symposium (International) on Combustion, Combustion Institute, Pittsburgh, 1969, pp. 85–211.
4. Thirteenth Symposium (International) on Combustion, Combustion Institute, Pittsburgh, 1971, pp. 495–572.
5. Putnam, A. A., *Combustion-Driven Oscillations in Industry*, Elsevier, N.Y., 1971.
6. Harrje, D. T. and Reardon, F. H. (eds), *Liquid Propellant Rocket Combustion Instability*, NASA SP-194, 1972.
7. Twentyfourth Symposium (International) on Combustion, Combustion Institute, Pittsburgh, 1992. For Candel's article, see pp. 1277–1296.
8. Twenthysixth Symposium (International) on Combustion, Combustion Institute, Pittsburgh, 1996, pp. 2803–2875.
9. Annaswamy, A. M. and Ghoniem, A. F., IEEE Control Systems Mag., 1995, Dec. issue, 49.
10. Raghu, S., Ph D thesis, Yale University, 1987.
11. Sreenivasan, K. R., Raghu, S. and Chu, B.-T., Shear Flow Conference, AIAA-85-0540, Boulder, CO, 1985.
12. Raghu, S. and Sreenivasan, K. R., Aeroacoustics Conference, AIAA-87-2690, Palo Alto, CA, 1987.
13. Rayleigh, Lord, *Theory of Sound*, Dover, 1945, vol. 2, section 322g, pp. 232–234.
14. Carrier, G. F., *Quart. Appl. Math*., 1954, **12**, 383.
15. Hussain, A. K. M. F. and Hasan, M. Z., *J. Fluid Mech*., 1983, **134**, 431.
16. Putnam, A. A. and Dennis, W. R., *J. Acoust. Soc. Am*., 1954, **26**, 716.
17. Tanida, Y., Okajima, A. and Watanabe, Y., *J. Fluid Mech*., 1973, **61**, 769.
18. Roquemore, W. M., Britton, R. L. and Sandhu, S. S., *AIAA J*., 1983, **21**, 1410.
19. Strykowksi, P. J. and Sreenivasan, K. R., Shear Flow Conference, AIAA-85-0559, Boulder, CO, 1985.

ACKNOWLEDGEMENTS. We wish to thank Prof. B.-T. Chu for his contributions to the work, Dr A. Annaswamy for bringing the *Wall Street Journal* article to our attention, and Mr I. San Gil for his help in scanning some of the figures.